

Brazil nut effect: Influence of friction and jamming on the transition line

P. Cordero*, S. Godoy*, D. Risso[†] and R. Soto*

*Departamento de Física, FCFM, Universidad de Chile, Santiago, Chile

[†]Departamento de Física, Facultad de Ciencias, Universidad del Bío-Bío, Concepción, Chile

Abstract.

We report a molecular dynamics study of the behavior of a bidimensional system consisting of a large disk (*the intruder*) immersed in a bed of many small disks. All collisions are instantaneous and inelastic and all possible parameters of the system are kept fixed except for two dimensionless parameters determining the frequency and amplitude of the vibrating base. A systematic exploration of this parameter space leads to determining a transition line separating a zone in which the *Brazil nut effect* is observed and one in which it is not. It is observed for the BNE to be present it is necessary that the characteristic velocity of the vibrating base is above a certain threshold. This threshold increases as the characteristic acceleration of the base gets larger. The results strongly suggest that, in the region of the parameter space in which the study is made, there is a minimum amplitude and a maximum frequency for the Brazil nut effect to take place. The shape of the transition line is understood in connection with the friction of the system with the lateral walls and with jamming. Friction with the lateral walls produces a net downward force, eventually leading to a convective current that pushes the intruder up. Although the energy injection rate, that helps the development of the convective current, is proportional mainly to the square of the velocity of the base, it is found that the average frictional force decreases when increasing the base acceleration. Therefore, for large base accelerations, higher values of the base velocity are needed to produce a convective current sufficiently strong. But if the system is not excited enough the friction which would produced convective currents are balanced by the reaction forces that result from jamming.

Keywords: granular systems, segregation

PACS: 45.70.-n, 45.70.Mg

INTRODUCTION

Granular matter, like sand, subjected to excitation may behave in peculiar ways. Much effort has been devoted for quite a while to understand its dynamics [1, 2, 3, 4, 5, 6]. When these systems are steadily excited they behave in several respects like a standard fluid but they exhibit some peculiar behavior of their own. Of the many phenomena that granular matter presents—under external excitations—one can mention the formation of clusters, avalanches, piling, pattern formation, sound propagation, and segregation. At present there is no generally accepted theory to anticipate how a granular system will behave under a given condition.

In this article we report a systematic molecular dynamic study of a bidimensional system of inelastic rough hard disks plus one larger particle, called *the intruder*. This system is in a box with vertical lateral walls subjected to a vertically vibrating base. Typically the intruder is initially placed at the bottom and, under appropriate conditions, it migrates to the top. This is the so called *Brazil nut effect* or BNE [7]. We have

published our first results on this in [8].

There is a similar, but different phenomenon, sometimes also called BNE, which does not have one intruder but rather it is a binary mixture, each species, typically occupying roughly the same volume. In the case of a binary mixture—differing by the size of the grains, or the density, etc—it is interesting to study the conditions under which the two species segregate and which species migrates to the top (BNE and reverse BNE), but, as said before, this case is different as it has additional effects involved such as the interactions among the large particles [9].

There are many experimental and simulational studies of segregation and in their conclusions authors attribute it to a variety of mechanisms such as: void filling [7, 10, 11], arch formation [12, 13, 14], percolation [15, 16], condensation [15, 16, 17], buoyancy [9, 18, 19, 20], inertia [20, 21], convection [13, 14, 20, 22, 23, 24, 25, 26] and competition between buoyancy and geometric forces [27, 28]. In Ref. [29] the authors tabulate seven possible mechanisms in the case when both types of grains have the same mass density.

The system we consider consists of N inelastic rough hard disks of mass m and diameter σ plus the intruder placed in a two dimensional box. All particles can rotate and their moment of inertia is that of filled disks, $m\sigma^2/8$. The base vibrates vertically with an amplitude A and an angular frequency ω . The lateral walls are rough and remain motionless; there is no top lid. As shown in Table 1 there are more than 20 dimensionless parameter in this class of problems. Obviously it is impossible to make a systematic experimental or simulational study covering this huge parameter space.

TABLE 1. The units are fixed by choosing the mass of the small particles as $m = 1$, the diameter of the small particles as $\sigma = 1$, and the acceleration of gravity as $g = 1$, hence the tabulated quantities can now be considered dimensionless. In principle, different values for the restitution and friction coefficients must be provided for disk-disk, disk-intruder, disk-wall, and intruder-wall collisions.

symbol	meaning	number	chosen value
N	number of small particles	1	1200
L_x	width of the box	1	40.0
σ_I	diameter of the intruder	1	8.0
r_n^i, r_t^i	restitution coefficients (normal and tangential)	8	0.98
μ_s^i, μ_d^i	friction coefficients (static and dynamic)	8	0.7
ρ_I/ρ_p	intruder's relative mass density	1	1.0
A, ω	amplitude and frequency of the base	2	free
TOTAL:		22	

In spite of the years the BNE has been studied experimentally or simulationally there is no generally successful theory to anticipate which mechanisms are dominant for the segregation phenomena neither it is understood under which specific conditions the intruder—or Brazil nut—would or would not rise to the top. Among the many difficulties are the many competing mechanism that exist and the huge parameter space where the phenomenon can be studied.

In what follows we fix most of these parameters to the values at the rightmost column in Table 1. In particular, the mass density of the intruder is the same as the small grains, and therefore heavier than the granular media, when the interstitial voids are considered. Hence buoyant forces would in principle make the intruder sink. To study the effects of the movement of the vibrating base, our only varying parameters are the amplitude and

angular frequency of the base: A and ω .

For numerical accuracy we do not use a sinusoidal function to define the movement of the base but a succession of parabolas. They are better adapted to the event driven molecular dynamics method used to simulate inelastic hard disks [30], $y_{\text{base}} = \frac{8A}{T^2}(2t - T)t$ if $0 \leq t < \frac{T}{2}$ while $y_{\text{base}} = \frac{8A}{T^2}(2t - T)(T - t)$ if $\frac{T}{2} \leq t < T$. This movement implies that the acceleration of the base is piecewise constant, $a_{\text{base}} = \pm \frac{32A}{T^2} = \pm \frac{8}{\pi^2} A \omega^2$. Instead of A and ω as our basic varying parameters we use the dimensionless acceleration and velocity of the base, which, as we show below better characterize the BNE

$$\Gamma = \frac{8}{\pi^2} \frac{A \omega^2}{g}, \quad \zeta = \sqrt{\frac{2}{\sigma g}} A \omega. \quad (1)$$

In terms of them the amplitude and frequency are of the form $A \propto \zeta^2/\Gamma$ and $\omega \propto \Gamma/\zeta$, namely fixing ζ , larger Γ implies smaller amplitude and higher frequency while fixing Γ , larger ζ implies larger amplitude and smaller frequency.

RESULTS

The transition line

In the region

$$2 \leq \Gamma \leq 12, \quad 1 \leq \zeta \leq 10 \quad (2)$$

we define a grid of points and for each point we have run three simulations—with different initial conditions and for at most 1500 cycles of the vibrating base—and have looked in each case whether the intruder rises above the center of mass of the small grains or not. In most points of the grid the three simulations give the same result, in the sense that the intruder rises to the top or it does not. There is a strip of points, however, where not all three simulations produced the same result. We call them *transition points*. We define a finer grid in that strip (more intermediate values of ζ for the values of Γ used before) and repeat the exercise of having three simulations per point. In total we make about 2000 simulations corresponding to about 650 points in the Γ - ζ plane. For each Γ we averaged the values of ζ for all the transition points, finding a set of values $\bar{\zeta}(\Gamma)$ for which we were able to adjust the following parabola

$$\zeta_{\text{trans}}(\Gamma) = (0.062 \pm 0.001)(\Gamma - 1)^2 + (1.84 \pm 0.06) \quad (3)$$

plotted at left in Fig. 1. We call it the *transition line* [8]. The Brazil nut effect is observed in the zone above the transition line, namely when $\zeta > \zeta_{\text{trans}}$. Marginally we mention that to obtain the fit presented above we included a term linear in $\Gamma - 1$ and its coefficient turned out to be smaller than its error bar.

Mapping the transition line to the ω - A plane, as shown at right in Fig. 1, it is seen that there is a maximum frequency beyond which there is no BNE and similarly there is a minimum amplitude below which again, there is no BNE. In both graphs of Fig. 1 the dashed line represents the direct extrapolation implied by Eq. (3).

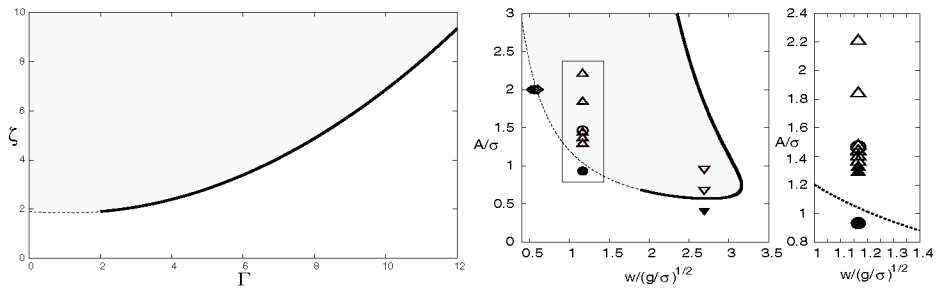


FIGURE 1. At left, in the Γ - ζ space is the transition line given by Eq. (3). In the explored region it is a solid line: above it (gray zone) the BNE is observed, below it it is not. At right the transition line drawn in the ω - A plane has the shape of a tongue. The darker part of the line corresponds to the explored region, the dashed line is the extrapolation based on the fit (3) and here too the gray part is where the BNE is observed. The shape of the curve clearly indicates that there is maximum frequency beyond which there is no BNE and similarly there is a minimum amplitude below which, again, there is no BNE. The symbols of different shapes represent the results obtained by different authors, as explained in the main text. Solid symbols refer to cases for which the BNE is observed within 1500 cycles of vibration of the base while open symbols imply that the BNE is not observed in that time. At the extreme right there is an enlargement of the rectangular zone of the main figure at right.

The existence of a maximum frequency may be due to the fact that the energy is injected mainly through the base in the form of a vibration and the penetration length of this energy flux decreases as the frequency of the base gets larger [31]. For high frequency the bottom part of the granular system gets excited while the rest of the system remains far from fluidized. The existence of a minimum amplitude will be discussed further on.

Friction with the lateral walls

It is quite clear—from looking at the animations of our simulation—that the BNE in the region we have studied is strongly determined by the convective current induced by the friction with the lateral walls.

Figure 2 shows that this force, on average, pushes down the grains colliding with the lateral walls. The lateral descending current in each side induces an ascending current in the middle of the box eventually making the intruder to move up. This asymmetry in the direction of the friction force is due to the behavior of the granular media in the different phases of the vibrating base. When the base is moving upwards the media is compressed increasing the lateral pressure, therefore increasing the frictional force; while when moving down the system is expanded with lower lateral pressure.

The averaged friction force is shown at left in Fig. 3 in the Γ - ζ plane. It is seen that for values of Γ smaller than about 3 the friction depends strongly on Γ and weakly on ζ . After an intermediate zone for frequencies above 2.5, the friction becomes almost ω -independent, becoming a decreasing function of the amplitude.

The energy injected through the vibrating base is roughly proportional to the average

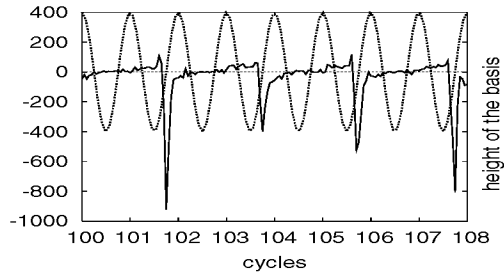


FIGURE 2. The force exerted on the particles of the system by friction with the lateral walls is plotted against the number of cycles of the vibrating base. The sinusoidal curve represents the height of the base in arbitrary units. This is the case $\Gamma = 4.1$ and $\zeta = 3.5$ for which the force oscillates with a period twice that of the vibrating base. The force is dominated by its negative values (downwards force) and it is seen that the maximum friction takes place when the base is moving up at maximum speed.

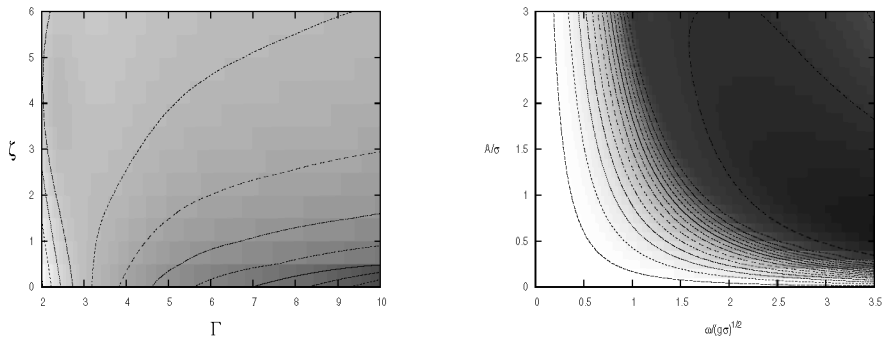


FIGURE 3. At left the iso-friction curves shown in this graph for $0 \leq \Gamma \leq 10$ and $0 \leq \zeta \leq 6$. Smaller values of the friction force is indicated with darker gray. For values of Γ smaller than about 3 it is seen that the friction is only weakly dependent on ζ . At right the iso-friction curves shown in the ω - A plane. For $\omega > 2.5$ the friction is almost independent of ω and for all values of this variable it is a decreasing function of the amplitude A .

of the square of its velocity, ζ^2 . Therefore the following argument can be made to understand the shape of the transition line. If the friction force produced by the two vertical walls—pushing the system downward—were independent of Γ , the transition line (at left in Fig. 1) would only depend on ζ , namely it should be a horizontal line. But, as already mentioned, the absolute value of the average friction force decreases as Γ grows (Fig. 3). Since when Γ gets larger the friction force is smaller (the engine to produce convection gets weaker), the system has to be more excited, more fluidized, (larger ζ) to allow for a convective current to exist. This suggests that the transition line $\zeta_{\text{trans}}(\Gamma)$ has to be a growing function as, in fact, implies Eq. (3). Marginally it should be mentioned that the friction with the walls implies a shear over the system and this

implies a secondary source of energy injection into the system.

Jamming

The conditions under which we are analyzing the behavior of the system correspond to configurations with quite large densities: there is crystalline order almost everywhere. There are long range position correlations and anisotropy: nothing like what is usually understood as a fluid [33]. In this context the role of crystallographic defects is a pending problem and in the following we simply describe what is observed.

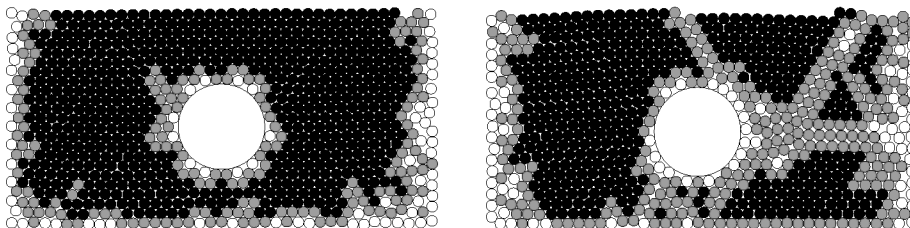


FIGURE 4. Bottom part of the system with $\Gamma = 4.5$, $\zeta = 2.5$ at left and with $\Gamma = 3.5$, $\zeta = 2.5$. at right. At left the final state after 3000 cycles which is seen to be quite ordered, while at right it is an early configuration of the case $\Gamma = 3.5$, $\zeta = 2.5$. Particles are colored according to how many close neighbors they have: black if there are 6 close neighbors; gray if there are 5 or 4 and white if there are 3 or less. This color encoding shows that at left the system is tightly packed almost everywhere while at right there are “channels” of lower density. More comments in the main text.

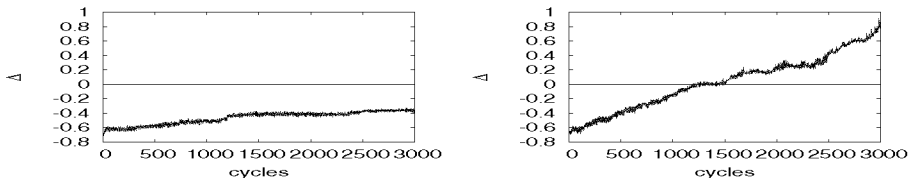


FIGURE 5. Both graphs show $\Delta \equiv (H_I - H_{cm})/H_{cm}$ against the number of cycles of the base, where H_I is the height of the intruder and H_{cm} is the height of the center of mass of the small particles. At left the case $\Gamma = 4.5$, $\zeta = 2.5$ while at right the case $\Gamma = 3.5$, $\zeta = 2.5$.

To understand the transition one has to consider that there are other forces which may prevent the intruder to moving up. In fact, our system is typically in configurations almost everywhere near closepacking: the densities observed, as in Fig. 4, are typically above 90% the closepacking density. Therefore all particles, in particular those in the neighborhood of the lateral walls, are being pushed not only by the walls but also by neighboring particles. If the system is not sufficiently excited it gets eventually jammed and no significant collective motion is observed for too long. Jamming in granular systems has been discussed in some detail for example in [32]

To illustrate the delicate balance that may trigger the intruder to move up let us compare two cases with $\zeta = 2.5$, one having $\Gamma = 4.5$ and the second one with $\Gamma = 3.5$. The evolution of the height of the intruder as a function of the number of cycles of the base in these two cases is shown in Fig.5. In the first case the intruder remains down

during the 3000 cycles that the system was simulated while in the second case, with $\Gamma = 3.5$, the intruder crosses the height of the center of mass after about 1300 cycles. It is interesting to compare the two snapshots shown in Fig. 4. At left is the lowest part of the configuration in the case $\Gamma = 4.5$, $\zeta = 2.5$ after 3000 oscillations of the base. The small particles form essentially a mono-crystal surrounding the intruder; there is no room for the intruder to move up since almost all the time the system remains this tight: it is jammed. The snapshot at right shows an early configuration in the case $\Gamma = 3.5$, $\zeta = 2.5$. It is seen that there are “channels” of lower density which keep changing as the system is adapting to the migration of the intruder to the top.

Comparison with other authors

There is a wide literature where the BNE is studied (see [5] for a complete review). It is, however, not trivial to decide which articles are suitable to compare with our results, in particular to validate our transition line Fig. 1. Scanning the large bibliography on the subject of BNE we decided to search for articles having simultaneously the following characteristics: presence of a single intruder, excitation via a vibrating base, lateral rough vertical walls, there is friction (some authors do MD without friction), the density of the intruder is the same as the other particles, either the amplitude of the base or its frequency are varied. We found only four articles shearing these properties: [13, 14, 22, 23]. Of these the only fully 3D experimental article is [22]. Its data can be seen in Fig. 3 represented by triangles pointing down: there is perfect consistent with our transition line; the other experimental article, [13] (data represented by circles in Fig. 3), makes a study in a quasi 2D case (a Helle-Shaw cell) and it shows a slight discrepancy with our curve. Something similar can be said of the other two (simulational) cited articles. Data from [23] are represented by rhombus and those from [14] are represented by triangles pointing up.

The extraordinary result of this comparison is that it shows almost perfect consistency between our transition line and the result of others in spite that in those studies the restitution and friction coefficients are different, the geometry is different, the number of particles is different and even the dimensionality of space is different. We cannot explain why, but it seems that our transition line has a validity far beyond its base of support.

PERIODIC BOUNDARY CONDITIONS

In the previous section it has been argued that friction with the lateral walls plays a central role in creating, via friction, a convective force pushing the system of small particles downwards, triggering two convective rolls which, if the effect is strong enough, induce an ascending current at the center of the box rising the intruder to the top. One should be tempted to conclude that if the lateral walls are replaced by periodic boundary conditions it would be impossible for the intruder to rise. This is true and false. If periodic boundary conditions are used while keeping the same values for all the other parameters and study the same region as before, in fact no BNE is observed. But at higher values

of Γ and ζ the BNE is observed. We have studied in particular the case $\zeta = 10$ and have seen that for $\Gamma \gtrsim 14.0$ there is BNE. This is the opposite to what was found in the previous sections in the sense that with rigid walls, fixing ζ , there is a value Γ_c such that above it *there is no* BNE, exactly the opposite of what happens in the present case. To make both cases consistent it seems necessary that the transition line in the Γ - ζ plane first rises, as we know, reaches a maximum and then starts to decrease. This is something that will have to be explored. Figure 6 shows the evolution of the height of the intruder and of the center of mass of the case $\Gamma = 15$ and $\zeta = 10$ with lateral periodic boundary conditions.

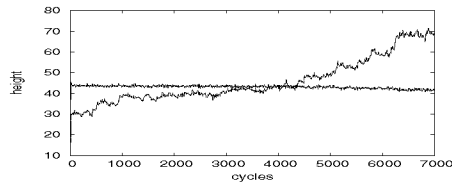


FIGURE 6. Height of the intruder and of the center of mass of the small particles in the periodic case with $\Gamma = 15$, $\zeta = 10$. Notice that the center of mass of the 1500 smaller particles moves down as the intruder moves up. The intruder reaches the top of the system in about 6000 oscillations of the base.

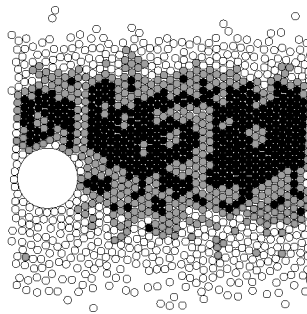


FIGURE 7. An intermediate configuration of the case $\Gamma = 15$, $\zeta = 10$ with periodic boundary conditions. It can be appreciated that in the lower part the system is gasified while in more than 2/3 of the rest it presents crystallographic order. The complete evolution of the height of the intruder in this case is given in Fig. 6. The use of gray is the same as in Fig. 4.

Having no walls to have friction with the typical ascending times that we have observed are much larger, which suggests that there are new and smaller effects which cause the BNE. The $\zeta = 10$ case that we have been looking at seems to be dominated by two effects depending on the height at which the intruder is. The small particles are so excited near the base that, as shown in Fig. 7, they are gasified, but starting at a height of about one third of the full height of the system the particles show crystalline order. This huge gradient in the granular temperature near the bottom implies a huge pressure gradient which forces the intruder in a very short time to higher and much denser regions. Hence the first effect is the pressure gradient. Higher up the intruder, being 16 times more massive than the small particles, behaves like a wall, in the sense that it pushes down the particles at its left or right sides. The asymmetry in the direction of the frictional force, described in the case of rigid walls (see Fig. 3), is preserved. Action and reaction implies

that the interaction with these lateral particles pushes the intruder up. The phenomenon is not simple and we are still trying to characterize it in detail. We observe that the intruder not only moves slowly up but it moves sideways as well. Apparently this horizontal component of its movement makes, during the lapse of several cycles, the convective current—pushing the small particles down—much stronger in one side of the intruder than in the other. This results in that the ascending movement of the intruder looks like a random zig-zag.

SUMMARY AND CONCLUSIONS

We have studied a system of 1200 disks of diameter $\sigma = 1$ plus an intruder of diameter $\sigma_I = 8$ in a box of width $L_x = 40$. The intruder has the same mass density as the smaller particles. We mainly describe the case when the vertical walls are rough and remain motionless while the base vibrates with amplitude A and angular frequency ω . Later we summarily describe the case when the lateral walls are replaced by periodic boundary conditions.

There is no upper lid. Initially the intruder is placed at the bottom while the base is at its highest position moving down. All the parameters characterizing the inelastic collisions (restitution and friction coefficients) are kept fixed to the values specified in Table 1. The only parameters used as control parameters are the dimensionless base acceleration Γ and velocity ζ , given by Eq. (1) in terms of A and ω .

In the case of rigid lateral walls the present study concludes that the main ingredients that determine the eventual migration of the intruder to the top are:

(a) The system has to be sufficiently excited to allow for rearrangement of particles. In the region we have explored these rearrangements, which can roughly be described as a “fluid” behavior, take place in spite of having densities not too far from closepacking. If the excitation is not large enough there is no significant collective movement and therefore no BNE can take place. The primary control parameter determining the energy input is ζ^2 and there is no BNE if ζ is smaller than about 1.9.

(b) The friction of the system with the lateral walls which produce, on average, a force pointing down on the system of small disks; this friction force, at fixed ζ , tends to be weaker for larger Γ . Eventually it produces a convective downwards convective current at both sides of the system, inducing an upward convective current in the middle of the system which may push the intruder to the top.

(c) Jamming. Since the density of the system of small particles is not too far from closepacking one can observe crystalline order almost everywhere. But this order may have many crystallographic defects, and they seem to play a crucial role. It is them which allow—now and then—the rearrangement of the small particles, hence diffusion, allowing the convective current to take place. If the system is not sufficiently excited by the vibrating base the system tends to have an order close to one single monocrystal. In such case jamming forbids any further collective motion except for the collective vibration of the whole system. There are no rearrangement and the intruder cannot migrate upward.

In the case when the lateral walls are replaced by periodic boundary conditions two effects are identified. In the region of the Γ - ζ plane where the BNE is observed with

periodic boundary conditions: near the bottom there is a strong pressure gradient pushing the intruder to the thick dense layer above. Once in that region the intruder itself acts as a rough wall pushing the small particles down, hence the intruder is boosted up.

ACKNOWLEDGMENTS

This research is supported by *Fondecyt* grants 1061112, 1070958 and *Fondap* grant 11980002.

REFERENCES

1. H. M. Jaeger, S. R. Nagel, *Science* **255** 1523 (1992).
2. H. M. Jaeger, S. R. Nagel and R. P. Behringer, *Rev. Mod. Phys.* **68** 1259 (1996).
3. L. P. Kadanoff, *Rev. Mod. Phys.* **71** 435 (1999).
4. P. G. de Gennes, *Rev. Mod. Phys.* **71**, 374 (1999).
5. A. Kudrolli, *Rep. Prog. Phys.*, **67**, 209 (2004).
6. R. Ramirez, D. Risso, and P. Cordero, *Phys. Rev. Lett.* **85**, 1230 (2000)
7. A. Rosato, K. J. Strandburg, F. Prinz, R. H. Swendsen, *Phys. Rev. Lett.* **58**, 1038 (1987).
8. S. Godoy, D. Risso, R. Soto and P. Cordero, *Phys. Rev. E* **78**, 031301 (2008).
9. D. A. Sanders, M. R. Swift, R. M. Bowley, P. J. King, *Phys. Rev. Lett.* **93**, 20, 208002 (2004).
10. R. Jullien, P. Meakin, A. Pavlovitch, *Phys. Rev. Lett.* **69**, 640 (1992).
11. S. Dippel, S. Luding, *J. Phys. I, France* **5**, 1527 (1995).
12. J. Duran, J. Rajchenbach, E. Clement, *Phys. Rev. Lett.* **70**, 2431 (1993).
13. J. Duran, T. Mazozi, E. Clement, J. Rajchenbach, *Phys. Rev. E* **50**, 5138 (1994).
14. A. Saez, F. Vivanco, F. Melo, *Phys. Rev. E* **72**, 021307 (2005).
15. D. C. Hong, P. V. Quinn, S. Luding, *Phys. Rev. Lett.* **86**, 3423 (2001).
16. A. P. J. Breu, H. M. Ensner, C. A. Kruelle, I. Rehberg, *Phys. Rev. Lett.* **90**, 1, 014302 (2003).
17. D. C. Hong, *Physica A* **271**, 192 (1999).
18. M. P. Ciamarra, M. D. DeVizia, A. Fierro, M. Tarzia, A. Coniglio, M. Nicodemi, *Phys. Rev. Lett.* **96**, 058001 (2006).
19. N. Shishodia, C. R. Wassgren, *Phys. Rev. Lett.* **87**, 084302 (2001).
20. D. A. Huerta and J. C. Ruiz-Suárez, *Phys. Rev. Lett.* **92**, 114301 (2004). *Phys. Rev. Lett.* **93**, 069901(E) (2004).
21. Y. Nahmad-Molinari, G. Canul-Chay, J. C. Ruiz-Suarez, *Phys. Rev. E* **68**, 041301 (2003).
22. J. B. Knight, H. M. Jaeger, S. R. Nagel, *Phys. Rev. Lett.* **70**, 3728 (1993).
23. T. Pöschel, H. J. Herrmann, *Europhys. Lett.* **29**, 123 (1995).
24. T. Shinbrot, F. J. Muzzio, *Phys. Rev. Lett.* **81**, 4365 (1998).
25. M. E. Möbius, B. E. Lauderdale, S. R. Nagel, H. M. Jaeger, *Nature* **414**, 270 (2001).
26. L. Vanel, A. D. Rosato, R. N. Dave, *Phys. Rev. Lett.* **78**, 7, 1255 (1997).
27. L. Trujillo, M. Alam and H.J. Herrmann, *Europhys. Lett.* **64**, 190 (2003).
28. M. Alam, L. Trujillo and H.J. Herrmann, *J. Stat. Phys.* **124**, 587 (2006).
29. M. Schröter, S. Ulrich, J. Kreft, J. B. Swift and H. L. Swinney, *Phys. Rev. E* **74**, 011307 (2006).
30. M. Marin, D. Risso and P. Cordero, *J. Comp. Phys.* **109**, 306 (1993)
31. R. Soto, *Phys. Rev. E* **69** 061305 (2004).
32. E. Corwin, H. Jaeger, S. Nagel, *Nature* **435**, 1075 (2005).
33. P. Cordero and D. Risso, *Physica A* **371**, 37-40 (2006)